Contents lists available at ScienceDirect

Journal of the Mechanical Behavior of Biomedical Materials

journal homepage: www.elsevier.com

Influence of crosslinking on the mechanical behavior of 3D printed alginate scaffolds: Experimental and numerical approaches

Saman Naghieh[a, *], Mohammad Reza Karamooz-Ravari[b], MD Sarker[a], Eva Karki[c], Xiongbiao Chen[a, d, *]

[a] Division of Biomedical Engineering, College of Engineering, University of Saskatchewan, Saskatoon, SK, Canada
[b] Department of Mechanical Engineering, Graduate University of Advanced Technology, 76318-18356 Kerman, Iran
[c] Department of Anatomy and Cell Biology, College of Medicine, University of Saskatchewan, Saskatoon, SK, Canada
[d] Department of Mechanical Engineering, College of Engineering, University of Saskatchewan, Saskatoon, SK, Canada

ARTICLE INFO

Keywords:
3D bioplotting
Crosslinking effect
Tissue scaffolds
Mechanical behavior
Elastic modulus
Numerical analysis

ABSTRACT

Tissue scaffolds fabricated by three-dimensional (3D) bioprinting are attracting considerable attention for tissue engineering applications. Because the mechanical properties of hydrogel scaffolds should match the damaged tissue, changing various parameters during 3D bioprinting has been studied to manipulate the mechanical behavior of the resulting scaffolds. Crosslinking scaffolds using a cation solution (such as $CaCl_2$) is also important for regulating the mechanical properties, but has not been well documented in the literature. Here, the effect of varied crosslinking agent volume and crosslinking time on the mechanical behavior of 3D bioplotted alginate scaffolds was evaluated using both experimental and numerical methods. Compression tests were used to measure the elastic modulus of each scaffold, then a finite element model was developed and a power model used to predict scaffold mechanical behavior. Results showed that crosslinking time and volume of crosslinker both play a decisive role in modulating the mechanical properties of 3D bioplotted scaffolds. Because mechanical properties of scaffolds can affect cell response, the findings of this study can be implemented to modulate the elastic modulus of scaffolds according to the intended application.

1. Introduction

Extrusion-based techniques are widely used to print large tissue scaffolds with cells and in such a system, biopolymers dispensed simultaneously from a 3D biofabrication system (Cao et al., 2012; Naghieh et al., 2018) and provide custom-made scaffolds using imaging technology (Naghieh et al., 2016a). It has also been combined with other techniques like electrospinning to come up with newly developed scaffolds (Naghieh et al., 2017a, 2017b). Such fabrication requires biocompatible bioink to maintain a hydrated environment essential for cell survival (Rajaram et al., 2014). Over the last decade, several hydrogel precursors have been investigated to develop suitable bioinks for extrusion-based systems (You et al., 2017). Seaweed-derived sodium alginate is a potential bioink for fabricating cell-incorporated 3D structures with remarkable geometric precision (Rajaram et al., 2015). In an extrusion-based biofabrication system, a cell-hydrogel precursor mixture is extruded layer-by-layer through a nozzle as per a pre-designed structure. The extruded alginate precursor must gel quickly to assist the fabrication process and support cell survival (Tripathi and Mishra, 2012; Yang et al., 2013). In this regard, divalent ionic crosslinkers have frequently been used to crosslink extruded hydrogel-based bioink because the ions cause rapid gelation and the gels can have acceptable printability and support the viability of any incorporated cells (Sarker and Chen, 2017).

Although alginate offers several attractive features for 3D biofabrication, the poor mechanical stability of alginate scaffolds has been a major issue that requires further investigation (Zhang et al., 2015). Several efforts have improved the mechanical stability of 3D alginate constructs. For instance, alginate composites have been explored but complexities associated with multi-polymer handling may limit their application (Naghieh et al., 2018). Other studies have been conducted to improve the mechanical stability of hydrogel scaffolds by manipulating the type and concentration of ionic crosslinkers (Hoffman, 2012). Among various divalent ions, Ca^{2+} ions facilitate superb printability for alginate precursors while maintaining reasonable cell viability (Swioklo et al., 2016). Mechanically stable alginate scaffolds can be successfully fabricated using $CaCl_2$ solution at higher concentrations (You et al., 2016a), but the incorporated cells can be adversely affected (Cao et al., 2012). Therefore, extruding the alginate precursor into a

* Corresponding authors.
Email addresses: san908@mail.usask.ca (S. Naghieh); xbc719@mail.usask.ca (X. Chen)

https://doi.org/10.1016/j.jmbbm.2018.01.034
Received 25 October 2017; Received in revised form 26 January 2018; Accepted 28 January 2018
Available online xxx
1751-6161/ © 2017.

UNCORRECTED PROOF

Influence of Crosslinking on the Mechanical Behavior of 3D Printed Alginate Scaffolds: Experimental and Numerical Approaches

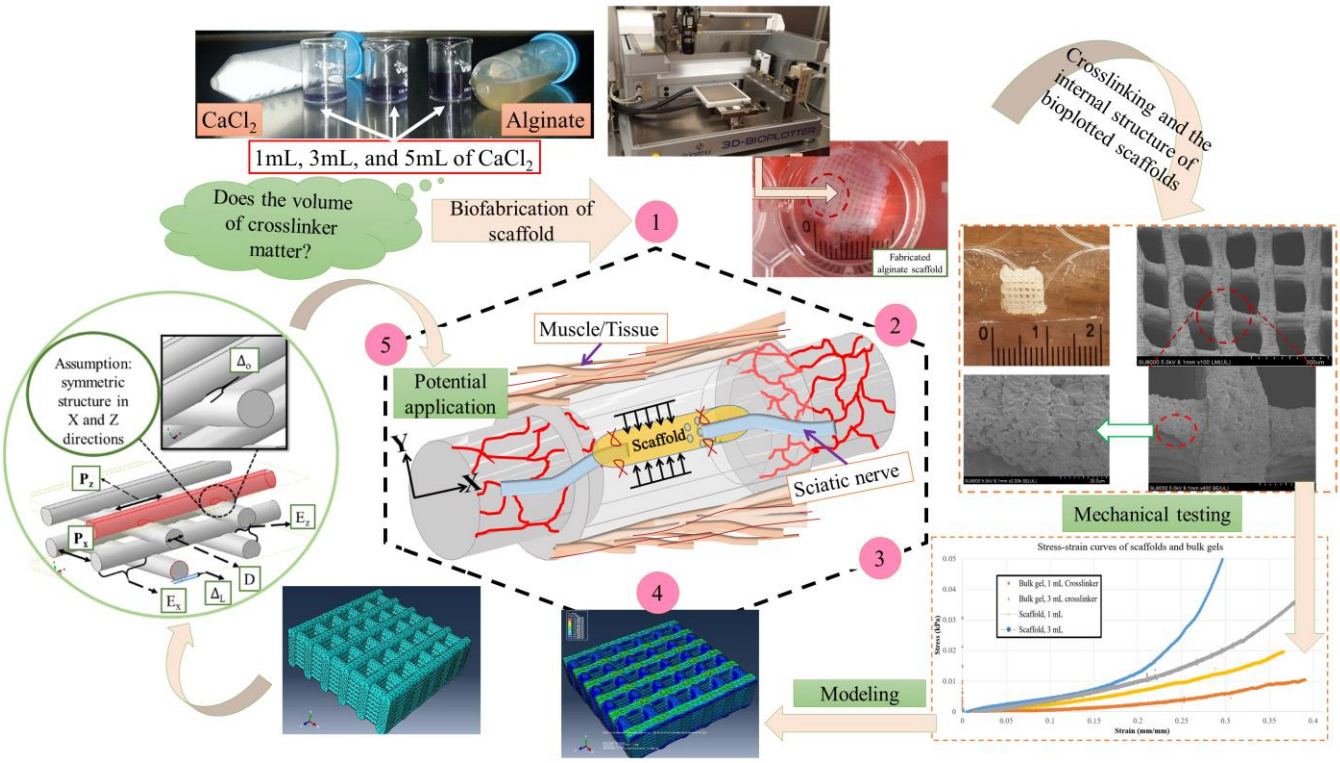

Author's Accepted Manuscript

Influence of Crosslinking on the Mechanical Behavior of 3D Printed Alginate Scaffolds: Experimental and Numerical Approaches

Saman Naghieh, Mohammad Reza Karamooz-Ravari, MD Sarker, Eva Karki, Xiongbiao Chen

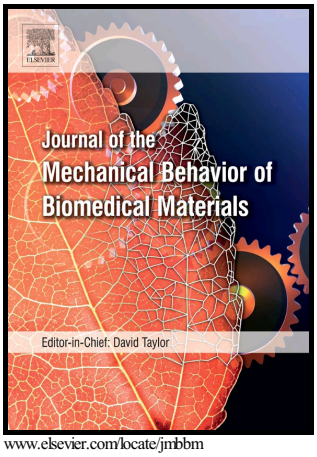

www.elsevier.com/locate/jmbbm

PII: S1751-6161(18)30047-X
DOI: https://doi.org/10.1016/j.jmbbm.2018.01.034
Reference: JMBBM2673

To appear in: *Journal of the Mechanical Behavior of Biomedical Materials*

Received date: 25 October 2017
Revised date: 26 January 2018
Accepted date: 28 January 2018

Cite this article as: Saman Naghieh, Mohammad Reza Karamooz-Ravari, MD Sarker, Eva Karki and Xiongbiao Chen, Influence of Crosslinking on the Mechanical Behavior of 3D Printed Alginate Scaffolds: Experimental and Numerical Approaches, *Journal of the Mechanical Behavior of Biomedical Materials,* https://doi.org/10.1016/j.jmbbm.2018.01.034

This is a PDF file of an unedited manuscript that has been accepted for publication. As a service to our customers we are providing this early version of the manuscript. The manuscript will undergo copyediting, typesetting, and review of the resulting galley proof before it is published in its final citable form. Please note that during the production process errors may be discovered which could affect the content, and all legal disclaimers that apply to the journal pertain.

Influence of Crosslinking on the Mechanical Behavior of 3D Printed Alginate Scaffolds: Experimental and Numerical Approaches

Saman Naghieh [1*], Mohammad Reza Karamooz-Ravari [2], MD Sarker [1], Eva Karki [3], Xiongbiao Chen [1,4*]

[1]Division of Biomedical Engineering, College of Engineering, University of Saskatchewan, Saskatoon, SK, Canada

[2]Department of Mechanical Engineering, Graduate University of Advanced Technology, 76318-18356 Kerman, Iran

[3]Department of Anatomy and Cell Biology, College of Medicine, University of Saskatchewan, Saskatoon, SK, Canada

[4]Department of Mechanical Engineering, College of Engineering, University of Saskatchewan, Saskatoon, SK, Canada

Abstract

Tissue scaffolds fabricated by three-dimensional (3D) bioprinting are attracting considerable attention for tissue engineering applications. Because the mechanical properties of hydrogel scaffolds should match the damaged tissue, changing various parameters during 3D bioprinting has been studied to manipulate the mechanical behavior of the resulting scaffolds. Crosslinking scaffolds using a cation solution (such as $CaCl_2$) is also important for regulating the mechanical properties, but has not been well documented in the literature. Here, the effect of varied crosslinking agent volume and crosslinking time on the mechanical behavior of 3D bioplotted alginate scaffolds was evaulated using both experimental and numerical methods. Compression tests were used to measure the elastic modulus of each scaffold, then a finite element model was developed and a power model used to predict scaffold mechanical behavior. Results showed that crosslinking time and volume of crosslinker both play a decisive role in modulating the mechanical properties of 3D bioplotted scaffolds. Because mechanical properties of scaffolds can affect cell response, the findings of this study can be implemented to modulate the elastic modulus of scaffolds according to the intended application.

Keywords

3D bioplotting; Crosslinking effect; Tissue scaffolds; Mechanical behavior; Elastic modulus; Numerical analysis

* Corresponding author at: Division of Biomedical Engineering, College of Engineering, University of Saskatchewan, Saskatoon, SK, Canada.

Email address: san908@mail.usask.ca, Tel: +1 306 966 5435 (S. Naghieh) and xbc719@mail.usask.ca, Tel.: 001-306-966-1267, Fax: 001-306-966-5427 (Xiongbiao Chen).

1. Introduction

Extrusion-based techniques are widely used to print large tissue scaffolds with cells and in such a system, biopolymers dispensed simultaneously from a 3D biofabrication system (Cao et al., 2012; Naghieh et al., 2018) and provide custom-made scaffolds using imaging technology (Naghieh et al., 2016a). It has also been combined with other techniques like electrospinning to come up with newly developed scaffolds (Naghieh et al., 2017a, 2017b). Such fabrication requires biocompatible bioink to maintain a hydrated environment essential for cell survival (Rajaram et al., 2014). Over the last decade, several hydrogel precursors have been investigated to develop suitable bioinks for extrusion-based systems (You et al., 2017). Seaweed-derived sodium alginate is a potential bioink for fabricating cell-incorporated 3D structures with remarkable geometric precision (Rajaram et al., 2015). In an extrusion-based biofabrication system, a cell-hydrogel precursor mixture is extruded layer-by-layer through a nozzle as per a pre-designed structure. The extruded alginate precursor must gel quickly to assist the fabrication process and support cell survival (Tripathi and Mishra, 2012; Yang et al., 2013). In this regard, divalent ionic crosslinkers have frequently been used to crosslink extruded hydrogel-based bioink because the ions cause rapid gelation and the gels can have acceptable printability and support the viability of any incorporated cells (Sarker and Chen, 2017).

Although alginate offers several attractive features for 3D biofabrication, the poor mechanical stability of alginate scaffolds has been a major issue that requires further investigation (Zhang et al., 2015). Several efforts have improved the mechanical stability of 3D alginate constructs. For instance, alginate composites have been explored but complexities associated with multi-polymer handling may limit their application (Naghieh et al., 2018). Other studies have been conducted to improve the mechanical stability of hydrogel scaffolds by manipulating the type and concentration of ionic crosslinkers (Hoffman, 2012). Among various divalent ions, Ca^{2+} ions facilitate superb printability for alginate precursors while maintaining reasonable cell viability (Swioklo et al., 2016). Mechanically stable alginate scaffolds can be successfully fabricated using $CaCl_2$ solution at higher concentrations (You et al., 2016a), but the incorporated cells can be adversely affected (Cao et al., 2012). Therefore, extruding the alginate precursor into a lower concentration $CaCl_2$ solution has been recommended to limit effects on cell viability (Tabriz et al., 2015). Cell-incorporated scaffolds should also be crosslinked immediately after printing to prevent significant decreases in cell viability (Cao et al., 2012). If the alginate precursor is extruded in a constant, low-concentration, and small volume of $CaCl_2$ solution, the number of available Ca^{2+} ions in the media might decline significantly with the progression of scaffold height; this, in turn, might affect the mechanical stability of the extruded hydrogel. Accordingly, an appropriate quantity of low concentration $CaCl_2$ solution should be employed in the biofabrication process to minimize the depletion effect of Ca^{2+} ions. However, this effect has not been thoroughly examined to date and so the appropriate volume and concentration of $CaCl_2$ solution required for an extrusion-based system without compromising the mechanical stability of the alginate scaffolds is not known.

Furthermore, extrusion-based biofabrication techniques require a specific amount of time to print a 3D structure and, during this period, scaffolds remain immersed in the crosslinker. Similar to concentration, crosslinking time in Ca^{2+} ions affects the viability of incorporated cells (Cao et al., 2012). In an extrusion-based system, the $CaCl_2$ solution is often aspirated upon biofabrication without allowing sufficient time for the alginate scaffolds to achieve equilibrium with the Ca^{2+} ions. While quick removal of the $CaCl_2$ solution improves cell viability, the mechanical stability of the alginate scaffolds could be significantly compromised. Scaffolds crosslinked for an extended

period could potentially be used for post-seeding applications, but the effect of immersing bioplotted alginate scaffolds in $CaCl_2$ solution for a prolonged period on the mechanical stability of the hydrogel construct has not been assessed.

This study investigated the volume of $CaCl_2$ and gelation time as potential significant parameters in the biofabrication process of alginate scaffolds. While some studies have focused on the concentration of crosslinker (Cao et al., 2012), here we exclusively concentrate on the effect of crosslinking time and volume for a fixed concentration of the crosslinking solution. The effect of these factors on the mechanical characteristics of the bioplotted scaffolds was investigated using experimental and numerical approaches. Alginate precursor was used as a bioink to print scaffolds with a 3D bioplotting machine. Bioink was extruded in $CaCl_2$ solution layer-by-layer to fabricate a cuboid structure. The gelation time was varied from 0 to 24 h, with the volume of 50 mM $CaCl_2$ solution maintained between 1 and 5 mL. The elastic modulus of the scaffolds produced was measured to evaluate the effect of varying volumes and gelation times of $CaCl_2$ solution, and then numerical models used to predict the elastic modulus of alginate scaffolds crosslinked with various volumes of crosslinker at a fixed concentration. Such models will be very useful for predicting the elastic modulus of alginate scaffolds *in situ* where the gelation time in the ionic crosslinkers must vary.

2. Materials and methods

2.1. Preparation of alginate solution and other required materials

Medium viscosity alginic acid sodium salt from brown algae (Sigma-Aldrich Canada Ltd., P-code 1001172534, with a molecular weight of 80,000-120,000 g/mol) was used for the preparation of a 3% w/v alginate solution using distilled water. Calcium chloride dehydrate (Sigma-Aldrich Canada Ltd., P-code 1001911753) was used for the preparation of a 50 mM $CaCl_2$ crosslinking solution. Tissue culture plates were treated with 0.5% (w/v) polyethylenimine (PEI, Alfa Aesar) and then incubated overnight at 37 °C and 5% carbon dioxide to improve the attachment of the first printed layer of alginate to the culture plate during the ensuing scaffold fabrication (Rajaram et al., 2015).

2.2. Design and fabrication of alginate scaffolds

The CAD model for scaffolds with dimensions of 10 × 10 × 5 mm was created using Magics EnvisionTEC (V13, Materialise, Belgium) and then sliced into 15 layers using Bioplotter RP software (V2.9, EnvisionTEC GmbH, Germany). The thickness of each layer was set at 160 µm and the distance between two adjacent strands at 1.5 mm.

A 3D bioplotter (EnvisionTEC GmbH) was used to fabricate the scaffolds with the alginate solution dispensed through a conical needle (EFD Nordson, Westlake, OH) with an inner diameter of 200 µm at a temperature of 20 °C. During dispensing, the applied pressure was set to 0.2 bar and the horizontal movement speed of the dispensing head to 6 mm/s. Scaffolds were fabricated layer-by-layer as per the CAD design by dispensing alginate solution into the wells of a 12-well tissue culture plate that held 1, 3, or 5 mL of 50 mM $CaCl_2$ as a crosslinking agent. Scaffolds were then either immediately subjected to mechanical testing or kept in the crosslinking solution at 37 °C for 2, 4, or 24 h before mechanical testing. The experimental groups are summarized in Table 1.

Table 1. Groups of scaffolds subjected to mechanical testing

Group	Crosslinking time in $CaCl_2$ upon fabrication (h)	Volume of $CaCl_2$ used for crosslinking (mL)	Storage temperature before mechanical testing (°C)
1	0	1	n/a
2	0	3	n/a
3	2	1	37
4	2	3	37
5	4	1	37
6	4	3	37
7	24	1	37
8	24	3	37
9	24	5	37

2.3. Mechanical testing

Compression tests were performed to calculate the elastic modulus of the scaffolds from the recorded stress-strain curves. To this end, a Bose BioDynamic^{TM} machine (with a load cell of 20 N) was used for compression tests on the scaffolds done at a speed of 0.01 mm/s (or a strain ratio of 0.0037 s^{-1}). Based on a method explained elsewhere (Naghieh et al., 2016b), the elastic modulus of the scaffolds was calculated using the linear section of the stress-strain curves and by defining the ε_0 (corrected zero strain point) as the intersection of the linear region of the curve and the zero-stress point (Figure 1). Compression tests were also performed on bulk alginate gels. Bulk gels were 3D bioplotted layer by layer to create an environment for their crosslinking similar to that used for the scaffolds (Figure 1a, b). The same volume of alginate used to create the scaffolds was used to fabricate the bulk gels. The elastic modulus values for the bulk gels were used to run the finite element model presented below.

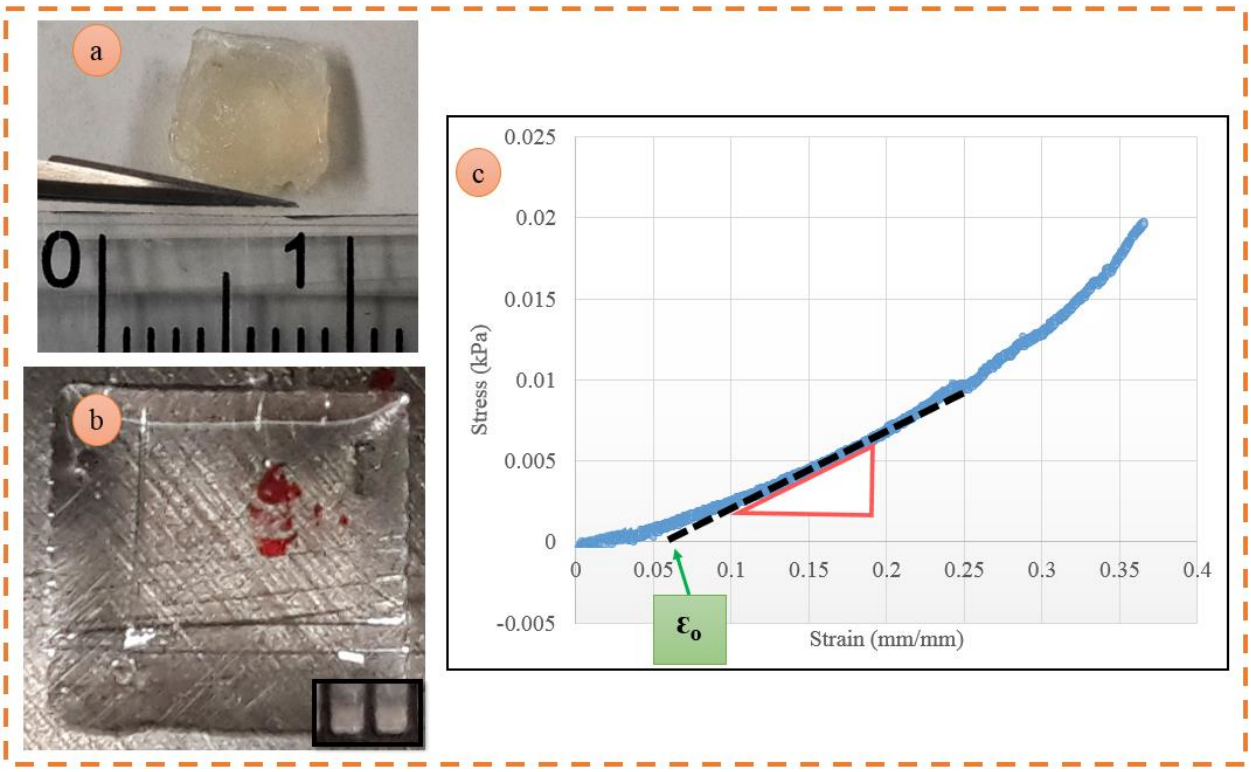

Figure 1. a) 3D bioplotted bulk gel, b) first printed layer of the bulk gel, and c) corrected stress-strain curve using corrected zero strain point

2.4. Numerical modeling of the linear/non-linear behavior of 3D bioplotted scaffolds

Two approaches were implemented to predict the mechanical behavior of 3D bioplotted scaffolds: linear elastic finite element modeling and non-linear regression modeling. The main goal of these numerical models are to predict the mechanical behavior of scaffolds prior to fabrication to optimize scaffold parameters pre-production, as producing various iterations for experimental characterization is costly and time consuming (Egan, 2017; Wieding et al., 2014).

To develop the linear finite element model, a Python script was developed using the finite element package ABAQUS 6.11-1. The proposed finite element model was developed to predict the elastic modulus of 3D bioplotted scaffolds immediately after printing. One of the inputs of this model is the elastic modulus of bulk gel, which can be affected by crosslinking time and volume; hence, the effect of crosslinking mechanism was taken into consideration. The details of the model developed are discussed elsewhere (Naghieh et al., 2016b, 2015). Briefly, scaffolds were considered as combinations of strands with 0° and 90° orientations and an interstrand distance representing the pore size in the X and Z directions. Figure 2 depicts the geometrical model used to define the structure of a 3D bioplotted scaffold. The number of strands (N) was chosen to represent the structure of the fabricated scaffolds and D was defined as the diameter of each strand. Additionally, the amount of penetration among layers (Δ_0) was considered in the model. According to the stress-strain curves of the compressed samples, the displacement of this elastic model was defined as 25%. A Poisson ratio of 0.31 was selected for alginate from the literature (Nguyen et al., 2009; Zhang et al., 2013) and Δ_L was defined as the value of deformed sections at the top and

bottom of the scaffold. Finally, E_x and E_z were defined in the model so that the real structure of the printed scaffold could be represented (Figure 2). Equations 1 to 3 were added to the developed Python script to mathematically represent the structure of the alginate scaffolds:

$$L_x = 2E_X + N_X D + (N_X - 1)P_X \qquad \text{Equation (1)}$$

$$L_Z = 2E_Z + N_Z D + (N_Z - 1)P_Z \qquad \text{Equation (2)}$$

$$L_y = \begin{cases} 2\left(\frac{D}{2} - \Delta L + N_{YZ}(D - \Delta_0)\right) & N_{YZ} = N_{YX} - 1 \\ 2\left(\frac{D}{2} - \Delta L + N_{YZ}(D - \Delta_0)\right) - (D - \Delta_0) & N_{YZ} = N_{YX} \end{cases} \qquad \text{Equation (3)}$$

where L_x, L_y, and L_z are dimensions of the scaffold in the X, Y, and Z directions, respectively. To reduce the computational effort, the model assumed symmetry in the X and Z directions and a strand diameter that was the mean of diameters measured from different points on the scaffold.

Ten-node modified quadratic tetrahedron elements with four integration points, denoted as C3D10 in ABAQUS, were used to mesh the model. The size of the mesh was initially set at 1 and then reduced until the change in the simulation results was negligible. Using this method, a mesh size of 0.3 was found appropriate and thus utilized for all simulations. Furthermore, the layer penetration was defined in the model as the amount of penetration of one layer into the next; full-attachment amongst layers was taken into account by merging nodes. Additionally, all geometrical features, i.e., pore size in different directions, strand diameter, thickness, etc., were obtained using captured images and added as model inputs. As such, the model considered all changes that might occur after printing, such as shrinkage, and was representative of the actual scaffolds fabricated.

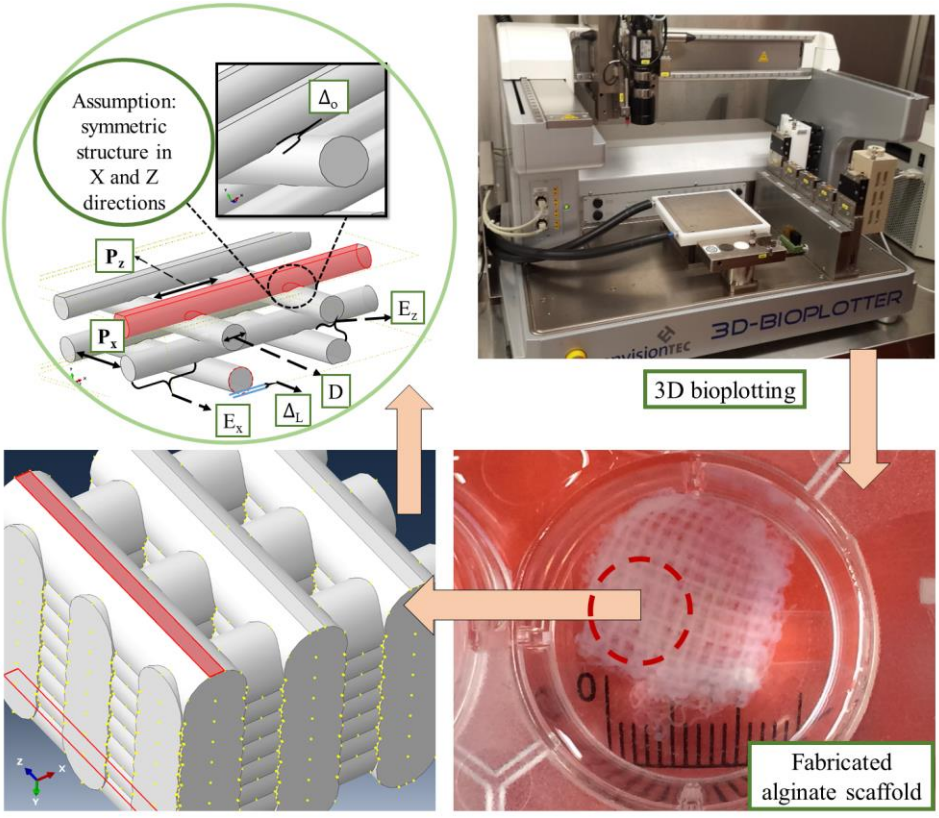

Figure 2. The model developed to represent the structure of the alginate scaffold fabricated using a 3D boiplotter: penetration within layers (Δ0), strand diameter (D), pore size in the X (Px) and Z (Pz) directions, exceeding distance after the last strand in X and Z directions (Ex and Ez), and the amount of deformation at the upper and lower sides of the scaffold (ΔL)

In addition, consideration of the nonlinear mechanical behavior of the scaffolds has been taken into account in many studies to date because the tissues being replaced by scaffolds are homogeneous materials with non-linear responses. Accordingly, a non-linear (empirical power) model was also developed to investigate the non-linear behavior of the bioplotted scaffolds and bulk gels. Power models have been widely reported in the literature for modeling the non-linear behavior of materials (Mancini et al., 1999), according to

$$6_E = K\varepsilon_E^n \qquad \text{Equation (4)}$$

where K is the rigidity constant (index of stiffness), n is the degree of concavity (index for the deviation from linearity), and σ_E, ε_E are stress and strain, respectively. For n=1, this equation is equal to Hooke's law and k represents the elastic modulus.

In some tissue engineering applications, such as peripheral nerve (Ning et al., 2016), bone (Naghieh et al., 2016b), and articular cartilage (You et al., 2016b) regeneration, scaffolds undergo compressive force exerted by over- and underlying tissues in one direction. In such cases, the compressive elastic modulus is important in one direction while the scaffold mechanical behavior in other directions might be different; indeed, bioprinted scaffolds are not isotropic (Olubamiji et al., 2016).

2.5. Imaging and morphology evaluation

Scanning electron microscopy (SEM) was used to investigate the scaffold morphology and open source software (ImageJ 1.5i) used to process the captured images.

2.6. Statistical analysis

All results are reported as mean values ± standard deviation. T-tests were used to compare the means of groups and determine statistical significance.

3. Results and discussion

3.1. Effect of the crosslinking time

Figure 3 shows the effect of crosslinking time on the elastic modulus of alginate scaffolds in a fixed volume (3 mL) of $CaCl_2$ crosslinker. Compression tests indicated elastic modulus values of 39.8 ± 6.36 kPa (immediately after printing), 99.3 ± 1.8 kPa (2 h after printing), 153.60 ± 16.10 kPa (4 h after printing), and 273.35 ± 5.55 kPa (24 h after printing). The larger elastic modulus observed with increasing time is attributed to more Ca^{+2} ions being involved in chemically crosslinking the alginate.

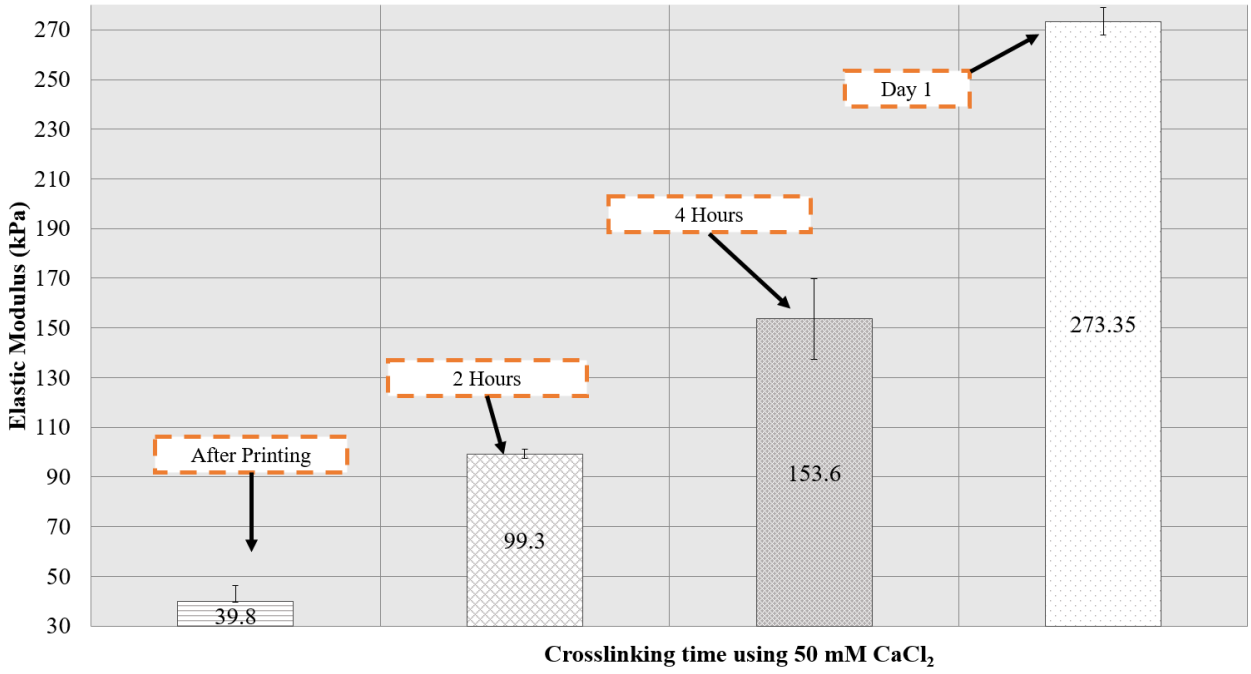

Figure 3. Effect of crosslinking time on the elastic modulus of alginate scaffolds immersed in 3 mL of 50 mM $CaCl_2$

3.2. Effect of crosslinker volume

Figure 4 shows the effect of varying the volume of $CaCl_2$ on the elastic modulus. The focus here was on the first 4 h after printing, which should provide sufficient time for the Ca^{+2} ions to penetrate the entire structure. As noted in §3.1 (see Figure 3), samples exposed to the crosslinking agent for a greater amount of time had a higher elastic modulus; for example, Figure 4 shows values of 21.65 ± 1.91 kPa immediately after printing vs. 80.25 ± 2.35 kPa measured 2 h later for scaffolds printed into 1 mL of $CaCl_2$. The elastic modulus of other samples with the same condition except for exposing to 3 mL of crosslinker agent was 39.8 ± 6.36 kPa, 99.3 ± 1.8 kPa, 153.60 ± 16.10 kPa, and 273.35 ± 5.55 kPa, as mentioned before. Comparing the mechanical properties of samples that were crosslinked in 1 vs. 3 mL of $CaCl_2$ for the same crosslinking time shows that a larger volume of crosslinking agent leads to better mechanical stability immediately after printing. Notably, samples crosslinked using either 3 or 5 mL of $CaCl_2$ had no significant difference in terms of elastic modulus after 24 h, which is attributed to the scaffolds reaching equilibrium with the crosslinking solution. For 3D bioplotting of cell-incorporated alginate scaffolds, crosslinking time is critical because cell viability can decrease significantly with exposure to the crosslinking solution (Cao et al., 2012). The results here indicate that the volume of crosslinker plays a decisive role in determining the elastic modulus of alginate scaffolds immediately after printing. These findings could be implemented to modulate the mechanical behavior of scaffolds to match those of the target tissue. In the next section, a finite element model is proposed to predict the elastic modulus of scaffolds immediately after printing.

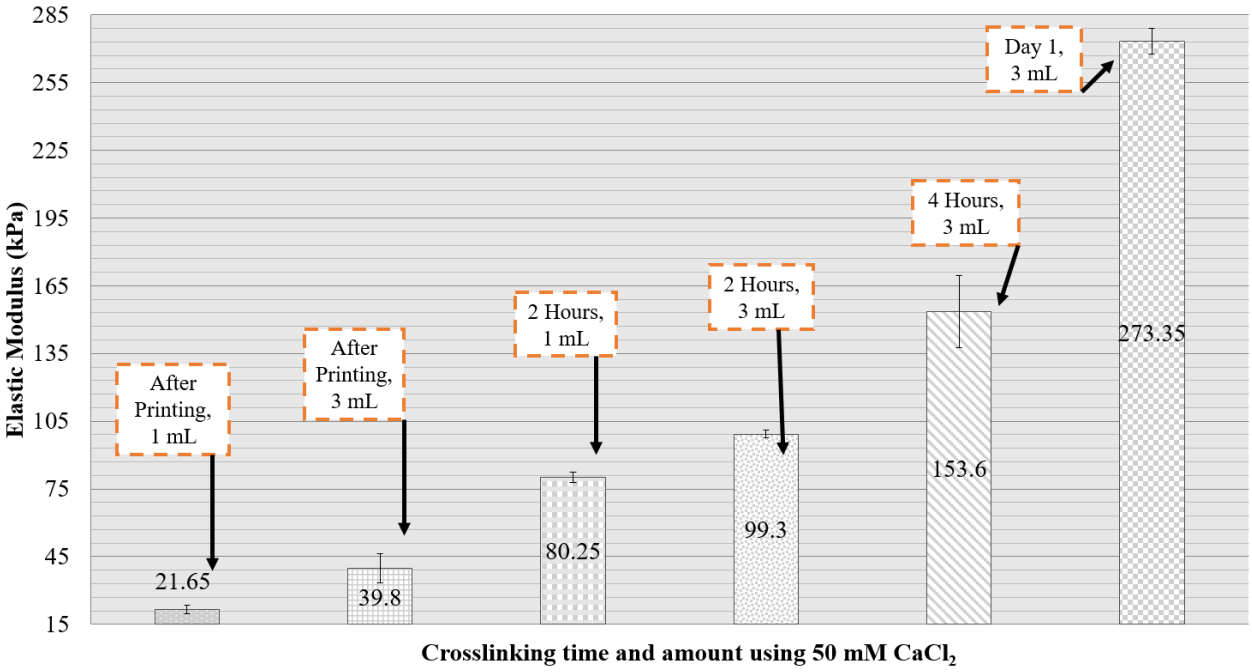

Figure 4. Effect of crosslinking time and crosslinker volume on the elastic modulus of alginate scaffolds immersed in 1 mL or 3 mL of crosslinking agent

3.3. Follow-up computational analysis

3.3.1. Linear elastic finite element model to predict the elastic modulus of scaffolds immediately after printing

A elastic linear model was developed to predict the elastic modulus of scaffolds exposed to 1 mL or 3 mL of crosslinker immediately after the 3D bioplotting process. As noted above, predicting the mechanical behavior of scaffolds immediately after printing would be useful for cell-incorporated scaffolds that cannot remain in crosslinking solution for a long time without compromising cell viability. To calculate the elastic modulus of the bulk materials, bulk alginate gels were exposed to 1 mL or 3 mL of crosslinker and immediately subjected to mechanical testing (data not shown). The significant difference between the elastic modulus of scaffolds crosslinked with 1 mL vs. 3 mL of crosslinker and compressed immediately after printing was shown in Figure 4; this is attributed to the porous structure of the scaffolds. SEM images of alginate scaffolds crosslinked for 24 h in 50 mM $CaCl_2$ indicate the presence of nanopores throughout the scaffold strands (Figure 5). These pores can increase the surface area and, consequently, more surface is exposed to the crosslinking agent. Hence, using 3 mL vs. 1 mL of crosslinker, and therefore more Ca^{2+} ions, can improve the mechanical stability of 3D bioplotted scaffolds immediately after printing.

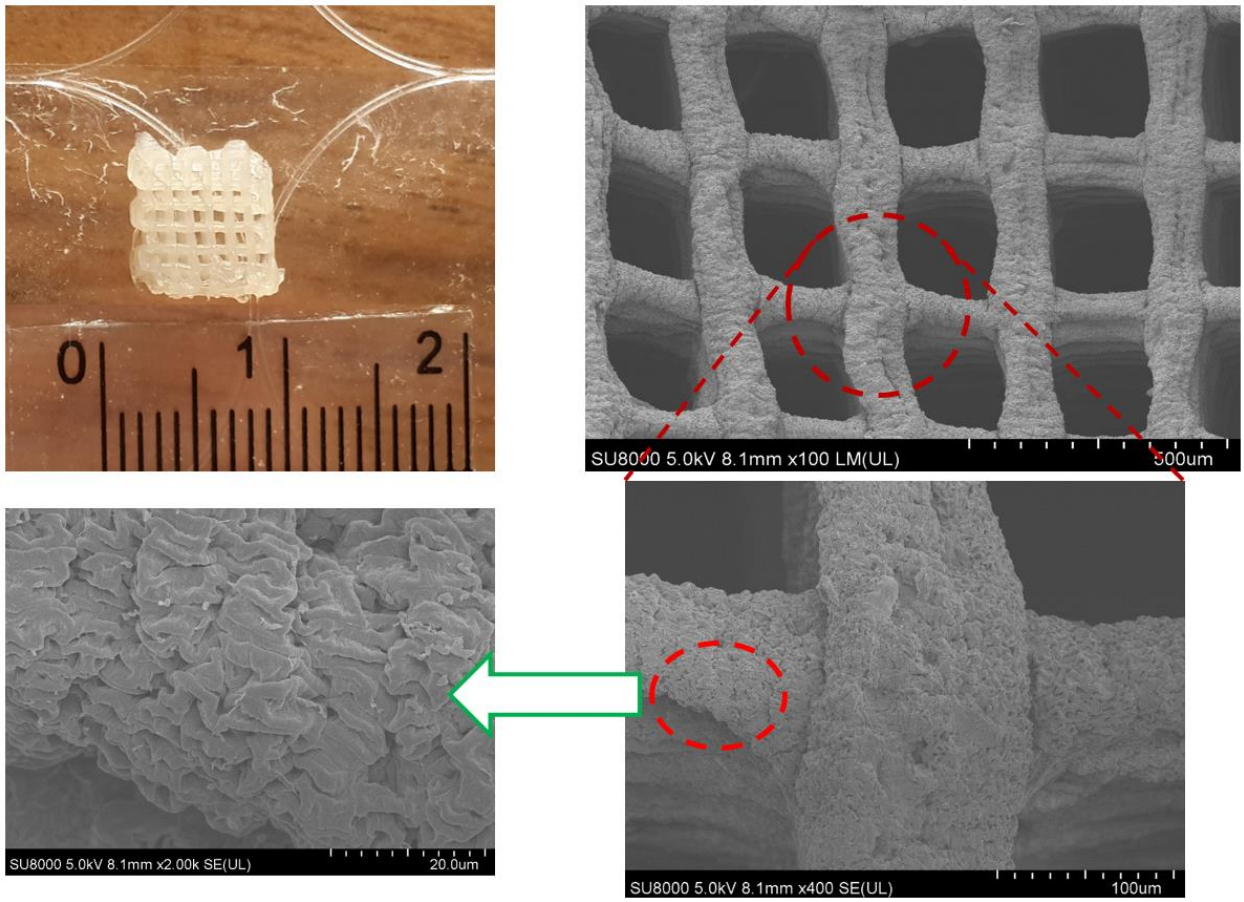

Figure 5. Morphology of bulk alginate gel (top left) and SEM images of an alginate scaffold immersed in 50 mM $CaCl_2$ for 24 h

Inputs for the linear elastic model were as follows. The elastic modulus values determined for the 3D bioplotted bulk gels immersed in 3 mL or 1 mL of $CaCl_2$ and subjected to mechanical testing immediately after printing were 79.2 ± 3.04 kPa (linear section, R^2=95.12%) and 42.3 ± 1.58 kPa (linear section, R^2=92.57%), respectively. Figure 6 demonstrates the stress-strain curves of the scaffolds and bulk gels, the boundary conditions applied in the model, the meshed part, and the collapsed scaffold after compression. The pore size (P=0.652 ± 0.04 mm), number of strands (N_X and N_Z=6, N_{YX}=7, N_{YZ}=8), diameter of each strand (D=0.516 ± 0.06 mm), amount of penetration among layers (Δ_0=0.392 mm), and the value of deformation (Δ_L=0.01 mm) were defined based on analyzing the images captured of the bioplotted scaffolds.

The model predicted an elastic modulus for scaffolds immersed in 3 mL of crosslinker and immediately subjected to compression testing of 38.59 kPa, which is in good agreement with values obtained experimentally (39.8 ± 6.36 kPa). Good agreement was also noted between the predicted elastic modulus of scaffolds immersed in 1 mL of crosslinker (20.58 kPa) and experimental results (21.65 ± 1.91 kPa).

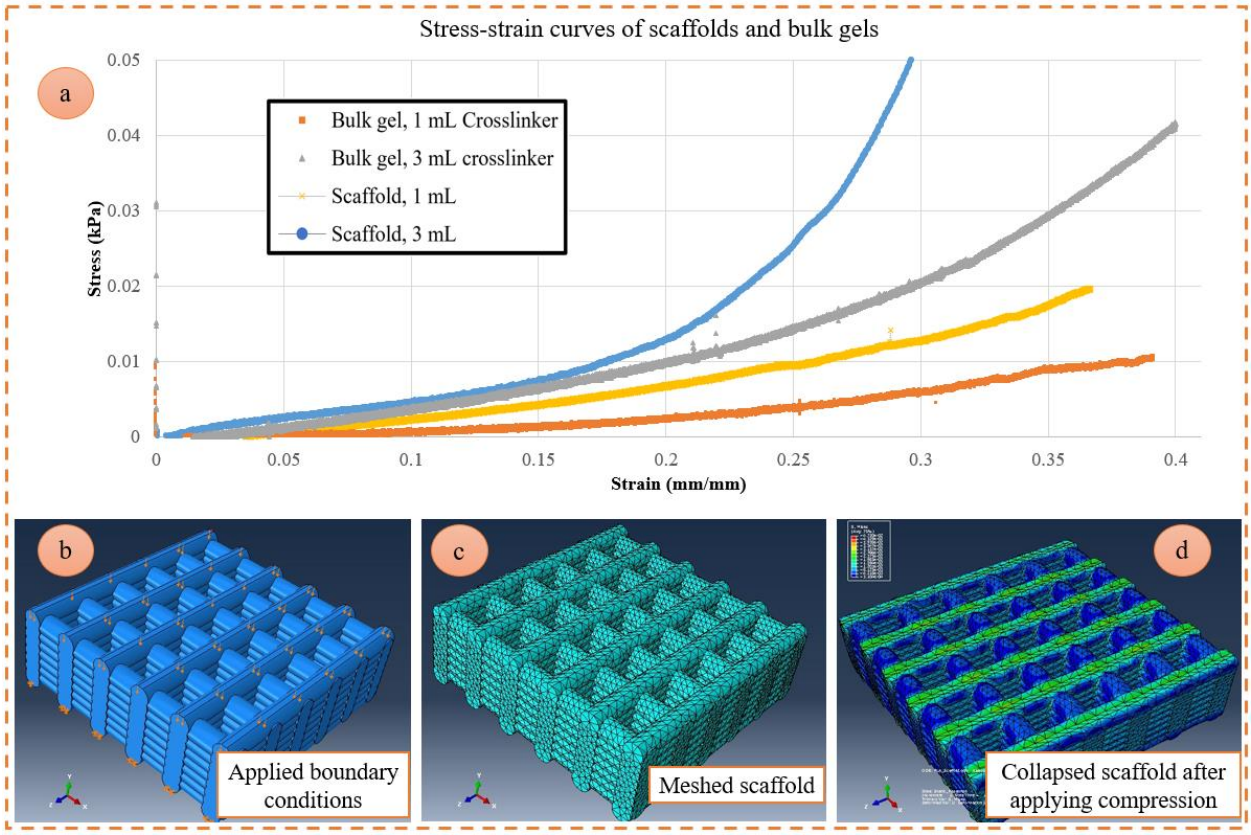

Figure 6. a) Stress-strain curves of alginate samples of scaffolds and bulk gels (compressed after 3D bioplotting), b) finite element model: I) applied boundary conditions, II) meshed part, and III) collapsed scaffold after compression

This linear elastic model might, therefore, be useful for predicting the elastic modulus of cell-incorporated scaffolds based on the relationship between crosslinking time and cell viability (Cao et al., 2012). Using the model developed, the volume of $CaCl_2$ crosslinker could be calculated in advance to modulate the mechanical properties of scaffolds so that the elastic modulus is matched according to the mechanical properties of the target tissue. As mentioned, the finite element model proposed only predicts the low-strain region of the stress-strain curve (linear elastic region). In some tissue engineering applications, such as nerve and skin regeneration, the linear, low-strain region of the stress-strain curve was used to calculate the elastic modulus of samples and considered to represent physiological behavior in the human vasculature (Amensag and McFetridge, 2014). In a similar study, isotropic linear elastic behavior was reported and 10% strain used to calculate the elastic modulus of scaffolds fabricated as cardiac-mimetic structures; furthermore, 10 to 25% strain was reported as the cardiac-relevant strain range in physiological conditions (Neal et al., 2012). Finally, a finite element study assigned linear elastic elements to a model to predict the mechanical properties of tissue-engineered cartilage constructs (Sengers et al., 2004). Hence, the direct determination of elastic modulus from the linear section of stress-strain curve is appropriate if the possible applications are taken into account. For example, cartilage undergoes loading and unloading with periodic stress relaxation. Therefore, the stress-strain curve is reproduced many times and determination of the elastic modulus from the linear section of a stress-strain curve of the material is appropriate. In the next, subsection, the non-linear behavior of biolpotted gels, as well as scaffolds, are investigated.

3.3.2. Non-linear numerical model to predict the non-linear behavior of 3D bioplotted scaffolds and bulk gels

The linear section of the stress-strain curve was predicted using the aforementioned linear elastic finite element model. Here, Equation 4 (empirical power model) was used to predict the non-linear behavior of scaffolds crosslinked for 24 h. The power model obtained for more than 50% strain was (R^2=96%):

$$\sigma_E = 0.126\varepsilon_E^{0.9917} \qquad \text{Equation (5)}$$

The n value of close to 1 (here 0.9917) in Equation 5 indicates the alginate behaves in a near linear elastic fashion according to Hooke's law. However, this equation demonstrates the dependency of the elastic modulus of alginate gels on the strain (strain-rate dependent behavior). Table 2 indicates the power models obtained for other samples at different times (immediately, 2h, and 4h after printing) and volumes (1 mL and 3 mL) of crosslinker. The majority of models have R^2 values greater than 90%, which indicates good agreement with experimental values. All also have n values larger than 1, which is evidence that they have completely non-linear behavior at higher values of strain. However, the proposed linear elastic finite element model (subsection 3.3.1) has utility for predicting the behavior of the scaffolds at lower values of strain, such as would be expected for the intended applications.

Table 2. Numerical models predicting the non-linear mechanical behavior of 3D bioplotted alginate gels and scaffolds

Crosslinker volume / Time	1 mL	3 mL
Gel: After printing	$\sigma_E = 0.0299\varepsilon_E^{1.4336}$ R^2 = 91%	$\sigma_E = 0.1986\varepsilon_E^{1.8158}$ R^2 = 97%
Gel: 2 hours	$\sigma_E = 0.0819\varepsilon_E^{1.1411}$ R^2 = 86%	$\sigma_E = 1.0137\varepsilon_E^{2.3338}$ R^2 = 90%
Gel: 4 hours	$\sigma_E = 0.3862\varepsilon_E^{1.7681}$ R^2 = 98%	$\sigma_E = 0.1264\varepsilon_E^{1.3187}$ R^2 = 96%
Scaffold: after printing	$\sigma_E = 0.0939\varepsilon_E^{1.6298}$ R^2 = 99%	$\sigma_E = 0.1437\varepsilon_E^{1.3866}$ R^2 = 92%

The power model $\sigma_E = 0.0939\varepsilon_E^{1.6298}$ (R^2=99%) was obtained for alginate scaffolds fabricated by the 3D bioplotting technique, crosslinked in 1 mL of $CaCl_2$, and subjected to mechanical testing immediately after printing (Table 2). The degree of concavity (n=1.6298) is greater than one and indicates non-linear behavior and an upward concavity, which is obvious from the stress-strain curve (Figure 6). Additionally, the rigidity constant for both the bulk gel and alginate scaffold is related to the alginate concentration, guluronic residue fraction, and viscosity. The alginate used in this study is composed of approximately 61% mannuronic acid and 39% guluronic acid (M/G ratio of 1.56), which under low strain behaves like an elastic material and

returns to its initial shape after removing the applied force. The power model for the scaffolds crosslinked in 3 mL of $CaCl_2$ and subjected to compression testing immediately after printing was $\sigma_E = 0.1437\varepsilon_E^{1.3866}$ (R^2=92%, Table 2).

Equation 6 was used to predict the stress at failure (σ_D, strength needed to break the material with a unitary surface), as reported by (Mancini et al., 1999):

$$\sigma_D = K\varepsilon_D^n \qquad \text{Equation (6)}$$

where σ_D and ε_D are the stress and strain at failure, respectively. Here, we considered 25% strain as the failure point for the scaffolds. Equation 6 predicted values of stress at failure of 9.8 kPa (1 mL $CaCl_2$) and 21.02 kPa (3 mL $CaCl_2$), which align well with experimental values of 9.77 kPa (1 mL $CaCl_2$) and 25.14 kPa (3 mL $CaCl_2$).

4. Conclusions

This study investigated the effect of crosslinking mechanism on the mechanical behavior of 3D bioplotted alginate scaffolds by varying the volume of 50 mM $CaCl_2$ crosslinker employed as well as the crosslinking time. Both immersion time and volume of crosslinker play a decisive role in modulating the elastic modulus of 3D bioplotted alginate scaffolds. These two previously unexplored factors can be used to modulate the mechanical properties of scaffolds to match those of the target tissue. Furthermore, numerical models (linear and non-linear) were developed to predict the elastic modulus of alginate scaffolds. The results from the models were in good agreement with experimental results and, as such, the models could be implemented to predict the mechanical properties of 3D bioplotted scaffolds.

Acknowledgments

The authors acknowledge financial support from the Natural Sciences and Engineering Research Council of Canada (NSERC, grant number RGPIN-2014-05648).

References

Amensag, S., McFetridge, P.S., 2014. Tuning scaffold mechanics by laminating native extracellular matrix membranes and effects on early cellular remodeling. J. Biomed. Mater. Res. Part A 102, 1325–1333.

Cao, N., Chen, X.B., Schreyer, D.J., 2012. Influence of Calcium Ions on Cell Survival and Proliferation in the Context of an Alginate Hydrogel. ISRN Chem. Eng. 2012, 1–9. doi:10.5402/2012/516461

Egan, P.F., 2017. PLOS ONE Computationally designed lattices with tuned properties for tissue engineering using 3D printing. PLoS One 12, 1–20. doi:10.1371/journal.pone.0182902

Hoffman, A.S., 2012. Hydrogels for biomedical applications. Adv. Drug Deliv. Rev. 64, 18–23.

Mancini, M., Moresi, M., Rancini, R., 1999. Mechanical properties of alginate gels: empirical characterisation. J. Food Eng. 39, 369–378.

Naghieh, S., Badrossamay, M., Foroozmehr, E., Kharaziha, M., 2017a. Combination of PLA Micro-fibers and PCL-Gelatin Nano-fibers for Development of Bone Tissue Engineering Scaffolds. Int. J. Swarm Intell. Evol. Comput. 6, 1–4. doi:10.4172/2090-4908.1000150

Naghieh, S., Foroozmehr, E., Badrossamay, M., Kharaziha, M., 2017b. Combinational processing of 3D printing and electrospinning of hierarchical poly(lactic acid)/gelatin-forsterite scaffolds as a biocomposite: Mechanical and biological assessment. Mater. Des. doi:10.1016/j.matdes.2017.07.051

Naghieh, S., Karamooz Ravari, M.R., Badrossamay, M., Foroozmehr, E., Kadkhodaei, M., 2016b. Numerical investigation of the mechanical properties of the additive manufactured bone scaffolds fabricated by FDM: The effect of layer penetration and post-heating. J. Mech. Behav. Biomed. Mater. 59, 241–250. doi:10.1016/j.jmbbm.2016.01.031

Naghieh, S., Ravari, M.R.K., Badrossamay, M., Foroozmehr, E., Kadkhodaei, M., 2015. Finite element analysis for predicting the mechanical properties of bone scaffolds fabricated by fused deposition modeling (FDM), in: Modares Mechanical Engineering, Proceedings of the Advanced Machining and Machine Tools Conference. pp. 450–454.

Naghieh, S., Reihany, A., Haghighat, A., Foroozmehr, E., Badrossamay, M., Forooghi, F., 2016a. Fused Deposition Modeling and Fabrication of a Three-dimensional Model in Maxillofacial Reconstruction. Regen. Reconstr. Restor. 1, 139–144. doi:http://dx.doi.org/10.22037/triple%20r.v1i3.12543

Naghieh, S., Sarker, M., Izadifar, M., Chen, X., 2018. Dispensing-based bioprinting of mechanically-functional hybrid scaffolds with vessel-like channels for tissue engineering applications – A brief review. J. Mech. Behav. Biomed. Mater. 78, 298–314. doi:10.1016/j.jmbbm.2017.11.037

Neal, R.A., Jean, A., Park, H., Wu, P.B., Hsiao, J., Engelmayr Jr, G.C., Langer, R., Freed, L.E., 2012. Three-dimensional elastomeric scaffolds designed with cardiac-mimetic structural and mechanical features. Tissue Eng. Part A 19, 793–807.

Nguyen, V.B., Wang, C.X., Thomas, C.R., Zhang, Z., 2009. Mechanical properties of single alginate microspheres determined by microcompression and finite element modelling. Chem. Eng. Sci. 64, 821–829. doi:10.1016/j.ces.2008.10.050

Ning, L., Xu, Y., Chen, X., Schreyer, D.J., 2016. Influence of mechanical properties of alginate-based substrates on the performance of Schwann cells in culture. J. Biomater. Sci. Polym. Ed. 27, 898–915.

Olubamiji, A.D., Izadifar, Z., Si, J.L., Cooper, D.M.L., Eames, B.F., Chen, D.X., 2016. Modulating mechanical behaviour of 3D-printed cartilage-mimetic PCL scaffolds: influence of molecular weight and pore geometry. Biofabrication 8, 25020. doi:10.1088/1758-5090/8/2/025020

Rajaram, A., Schreyer, D., Chen, D., 2014. Bioplotting Alginate / Hyaluronic Acid Hydrogel Scaffolds with Structural Integrity and Preserved Schwann Cell Viability. 3D Print. 1, 194–203. doi:10.1089/3dp.2014.0006

Rajaram, A., Schreyer, D.J., Chen, D.X.B., 2015. Use of the polycation polyethyleneimine to improve the physical properties of alginate–hyaluronic acid hydrogel during fabrication of tissue repair scaffolds. J. Biomater. Sci. Polym. Ed. 26, 433–445.

Sarker, M., Chen, X.B., 2017. Modeling the Flow Behavior and Flow Rate of Medium Viscosity Alginate for Scaffold Fabrication With a Three-Dimensional Bioplotter. J. Manuf. Sci. Eng. Trans. ASME 139. doi:10.1115/1.4036226

Sengers, B.G., Van Donkelaar, C.C., Oomens, C.W.J., Baaijens, F.P.T., 2004. The local matrix distribution

and the functional development of tissue engineered cartilage, a finite element study. Ann. Biomed. Eng. 32, 1718–1727.

Swioklo, S., Ding, P., Pacek, A.W., Connon, C.J., 2016. Process parameters for the high-scale production of alginate-encapsulated stem cells for storage and distribution throughout the cell therapy supply chain. Process Biochem.

Tabriz, A.G., Hermida, M.A., Leslie, N.R., Shu, W., 2015. Three-dimensional bioprinting of complex cell laden alginate hydrogel structures. Biofabrication 7, 45012. doi:10.1088/1758-5090/7/4/045012

Tripathi, R., Mishra, B., 2012. Development and evaluation of sodium alginate–polyacrylamide graft–co-polymer-based stomach targeted hydrogels of famotidine. AAPS PharmSciTech 13, 1091–1102.

Wieding, J., Wolf, A., Bader, R., 2014. Numerical optimization of open-porous bone scaffold structures to match the elastic properties of human cortical bone. J. Mech. Behav. Biomed. Mater. 37, 56–68.

Yang, C.H., Wang, M.X., Haider, H., Yang, J.H., Sun, J.-Y., Chen, Y.M., Zhou, J., Suo, Z., 2013. Strengthening alginate/polyacrylamide hydrogels using various multivalent cations. ACS Appl. Mater. Interfaces 5, 10418–10422.

You, F., Eames, B.F., Chen, X., 2017. Application of Extrusion-Based Hydrogel Bioprinting for Cartilage Tissue Engineering. Int. J. Mol. Sci. 18, 1597.

You, F., Wu, X., Zhu, N., Lei, M., Eames, B.F., Chen, X., 2016a. 3D Printing of porous cell-laden hydrogel constructs for potential applications in cartilage tissue engineering. ACS Biomater. Sci. Eng. 2, 1200–1210.

You, F., Wu, X., Zhu, N., Lei, M., Eames, B.F., Chen, X., 2016b. 3D Printing of Porous Cell-Laden Hydrogel Constructs for Potential Applications in Cartilage Tissue Engineering. ACS Biomater. Sci. Eng. 2, 1200–1210. doi:10.1021/acsbiomaterials.6b00258

Zhang, Y., Liu, J., Huang, L., Wang, Z., Wang, L., 2015. Design and performance of a sericin-alginate interpenetrating network hydrogel for cell and drug delivery. Sci. Rep. 5, 12374.

Zhang, Y., Yu, Y., Chen, H., Ozbolat, I.T., 2013. Characterization of printable cellular micro-fluidic channels for tissue engineering. Biofabrication 5, 25004. doi:10.1088/1758-5082/5/2/025004

Figure captions

Figure 1. a) 3D bioplotted bulk gel, b) first printed layer of the bulk gel, and c) corrected stress-strain curve using corrected zero strain point

Figure 2. The model developed to represent the structure of the alginate scaffold fabricated using a 3D boiplotter: penetration within layers (Δ_0), strand diameter (D), pore size in the X (P_x) and Z (P_z) directions, exceeding distance after the last strand in X and Z directions (E_x and E_z), the amount of deformation at the upper and lower sides of the scaffold (Δ_L)

Figure 3. Effect of crosslinking time on the elastic modulus of alginate scaffolds immersed in 3 mL of 50 mM $CaCl_2$

Figure 4. Effect of crosslinking time and crosslinker volume on the elastic modulus of alginate scaffolds immersed in 1 mL and 3 mL of crosslinking agent

Figure 5. Morphology of bulk alginate gel (top left) and SEM images of an alginate scaffold immersed in 50 mM $CaCl_2$ for 24 h

Figure 6. a) Stress-strain curves of alginate samples of scaffolds and bulk gels (compressed after 3D bioplotting), b) finite element model: I) applied boundary conditions, II) meshed part, and III) collapsed scaffold after compression

Table captions

Table 1 . Groups of scaffolds subjected to mechanical testing

Table 2. Numerical models predicting the non-linear mechanical behavior of 3D bioplotted alginate gels and scaffolds